

Journal of Mechanics of Materials and Structures

**TUNING THE PROPAGATION CHARACTERISTICS OF THE TRAPPED
AND RELEASED STRONGLY NONLINEAR SOLITARY WAVES
IN 1-D COMPOSITE GRANULAR CHAIN OF SPHERES**

Bin Wu, Heying Wang, Xiucheng Liu, Mingzhi Li, Zongfa Liu and Cunfu He

Volume 14, No. 3

May 2019



TUNING THE PROPAGATION CHARACTERISTICS OF THE TRAPPED AND RELEASED STRONGLY NONLINEAR SOLITARY WAVES IN 1-D COMPOSITE GRANULAR CHAIN OF SPHERES

BIN WU, HEYING WANG, XIUCHENG LIU, MINGZHI LI, ZONGFA LIU AND CUNFU HE

After a chain composed of light particles is inserted into a one-dimensional heavy granular chain of spheres, the formed composite chain can trap strongly nonlinear solitary waves (SNSWs) in a light sectional chain. The light sectional chain can reduce the peak amplitude of pulse waves imposed on the objects contacting with the end particle of the chain. However, the effects of the light sectional chain's properties on the propagation velocity and amplitude of both the trapped and output pulse waves are unclear. In this study, finite element models with optimal parameters were established to investigate the multireflection behaviors of the output pulse waves. Both the simulation and experimental results demonstrated that the light sectional chain could act as a physical regulator to tune the properties of the output pulse waves in the composite chain. When the material of the light particle was fixed, both the propagation velocity and amplitude of the output pulse waves exhibited the exponentially downward trend as the number of light particles increased. Compared to the light sectional chain of Brass, the PTFE chain could cause more serious attenuation on the amplitude of the pulse waves and reduce the propagation velocity of the output pulse waves. Similar phenomena had been reported in simulation results only at the nanoscale. Even at the macroscale, the investigated composite chain could quantitatively tune the propagation characteristics of the trapped and output pulse waves by adjusting the material and number of light particles.

1. Introduction

Strongly nonlinear solitary waves (SNSWs), which are derived from the nonlinearity of the Hertzian contact interactions between spherical particles, in one-dimensional granular chains have been widely explored due to the unique properties [Nesterenko 1983; Daraio et al. 2006a; Potekin et al. 2013; Nesterenko et al. 2005], such as independence of their width on amplitude and strong dependence of speed on amplitude. Wave dynamics in one-dimensional granular chains have been extensively investigated in the last twenty years to reveal the behavior of wave propagation in the granular chains and various potential applications have been reported, such as the design of metamaterials and metadevices [Gantzounis et al. 2013; Kim et al. 2017; Xu and Nesterenko 2017; Raney et al. 2016], nondestructive material evaluations [Rizzo et al. 2015], energy harvesting [Li and Rizzo 2015a; 2015b; Rizzo and Li 2017], and even medical hyperthermia [Spadoni and Daraio 2010]. The effects of particle material properties and impact condition on the formation and propagation velocity of SNSWs supported by 1-D chain of homogeneous elastic spherical particles have been reported [Meidani et al. 2015; Ngo et al. 2011; 2013; Khatri et al. 2012].

Keywords: 1-D composite granular chain, strongly nonlinear solitary waves, propagation characteristics tuning, energy trapping.

To reveal the wave propagation behavior in granular chains subjected to external impact, Nguyen and Brogliato [2014] and Brogliato [2016] published monographs to introduce and summarize the available theoretical approaches and computation tools. Theoretical expression about the energetical coefficient of restitution related with plastic (residual) indentation are first given in [Nguyen and Brogliato 2014]. Further study was reported by Zhao et al. [2008] to clarify the wave behavior in a column of beads colliding against a wall through adjusting the energetical restitution coefficient of a bistiffness compliant contact model. Falcon et al. [1998] found that spheres could be modelled as rigid bodies with localized deformation based on the Hertz' elasticity at the contact points. Kuninaka and Hayakawa [2009] partially determined dissipation during binary collision of nanoparticles through molecular dynamics and macroscopic collision model. Takato et al. [2018] obtained inelastic contact force between nanoparticles based on Hertz contact mechanics by molecular dynamics model. Many finite element methods had been developed to simulate the propagation properties of waves in one-dimensional particle chains [Musson and Carlson 2014; 2016; Ngo et al. 2011; Kim et al. 2015] since the attenuation caused by the plastic deformation generated between contacting particles could be calculated more accurately [Musson and Carlson 2014; 2016].

The composite granular chain with multisectional chains of spherical particles endows pulse waves with certain propagation characteristics [Przedborski et al. 2015; Vergara 2005; Hong and Xu 2002] and can act as a container to trap the energy of pulse waves in a particular section of chain [Nesterenko et al. 1995; Daraio et al. 2006b; Sen et al. 2008; Carretero-González et al. 2009]. In a composite granular chain of spherical particles, which is divided into two heavy sections and one light section, the leakage of trapped energy demonstrates a power-law behavior over time [Hong 2005; Wang et al. 2007; Xu and Zheng 2017]. The power-law behavior of the trapped energy release is attributed to the back-and-forth reflection of the sequence of pulse waves bouncing between the heavy-light and light-heavy interfaces. The bouncing behavior of the output pulse waves predicted by the theoretical model [Xu and Zheng 2017; Khatri 2012] was not confirmed or discussed by experimental tools yet. In addition, no dissipation on collisions is taken into account, so it is predicted that the output pulse waves move freely in the light section of chain without energy dissipation. The prediction remains to be experimentally explored.

Daraio et al. [2006b] experimentally investigated the reflection and transmission behaviors of pulse waves at the interface between steel particle and PTFE particle in composite granular chains. When pulse waves passed through heavy steel particles and entered the light PTFE section of chain, pulse waves decompose into a sequence of solitary waves with slower velocity and lower amplitude than that of incident pulse waves. In the design of a fine granular protector, the amplitude of the final output pulse waves of the composite granular chain is more concerned, but the energy dissipation and velocity variation of pulse waves in the light chain are seldom considered [Daraio et al. 2006b]. The effect of the number of particles in the light chain on the features of output pulse waves is still unknown.

The behavior of solitary waves propagating along the light section of chain in 1-D composite granular chain constructed by inserting a series of short single-walled carbon nanotubes into C_{60} system was simulated at the nanoscale [Xu and Zheng 2017]. A concept of energy tunnel was proposed based on the truth that both the propagation velocity and the energy carried by the solitary waves continuously decayed as the number of the carbon nanotubes increased. The interesting phenomenon of energy tunnel arose from the increase in the internal energy in carbon nanotubes with the consumption of the energy

of solitary waves passing through carbon nanotubes, but the phenomenon had not been verified at the macroscale [Xu and Zheng 2017].

Therefore, in this study, it is hypothesized that the energy tunnel phenomenon occurs in 1-D composite granular chain of particles at the macroscale. Both the finite element simulation and proof-of-concept experiments were performed to investigate the propagation characteristics of the trapped and output pulse waves in 1-D composite granular chain of particles. The simulation and experimental results confirmed the hypothesis. During the propagation of output pulse waves in the light sectional chain, the propagation velocity of pulse waves successively decreased due to the accumulation effect of the deformation energy storage. As the number of light particles increased, both the propagation velocity and amplitude of the output pulse waves in the end heavy chain demonstrated the exponentially downward trend.

This paper is organized as follows. In Section 2, based on Hertzian contact theory, the pulse waves in 1-D composite granular chain of spheres as well as the reflections of the output pulse waves are introduced. In Section 3, finite element models are established and the parameters of the models are optimized. The propagation characteristics of the trapped and output pulse waves is numerically investigated and discussed. In Section 4, the experimental setup is presented and simulation results are compared with experimental results. Finally, the conclusion is drawn in Section 5.

2. Fundamental theory

One-dimensional granular chain is a collection of macroscopic discrete particles whose dimensions are comparable to those of the overall system and so large that the thermal motion of particles may be ignored [Nesterenko 1983]. In a monatomic granular chain composed of N spherical particles shown in Figure 1 (top), the applied static force F_0 results in a small deformation at the contact area of adjacent particles and a relative displacement of δ_0 between the centers of two adjacent particles is generated. Under the action of an external impact F_d imposed along the particle alignment direction, the displacement of the center of individual particle is u_n ($n = 1, 2, \dots, N$). If the chain is uncompressed ($F_0 = 0$) or weakly precompressed ($F_0 \ll F_d$, resulting in $|u_{n+1} - u_n|/\delta_0 \gg 1$), the formation of strongly nonlinear solitary waves (SNSWs) in the chain is dominated by Hertzian contact law due to the balance of dispersion and interparticle nonlinearity. The contact force F between two adjacent particles is expressed as [Hertz 1881; Nesterenko 2001]

$$F(\delta) = \begin{cases} A\delta^{3/2}, & \delta > 0 \\ 0, & \delta < 0, \end{cases} \quad (1)$$

where δ represents the relative displacement of the centers of two adjacent particles. The contact stiffness A during compression can be calculated as [Nesterenko 2001]

$$A = \frac{4E_1E_2(1/R_1 + 1/R_2)^{-1/2}}{3[E_2(1 - \nu_1^2) + E_1(1 - \nu_2^2)]},$$

where R_1 and R_2 are the radii of the particles, and E_1 , E_2 , ν_1 , and ν_2 are Young's modulus and Poisson's ratio of the two particles' material, respectively. The motion equation for each particle is

$$\ddot{u}_n = A(\delta_0 - u_n + u_{n-1})^{3/2} - A(\delta_0 - u_{n+1} + u_n)^{3/2}. \quad (2)$$

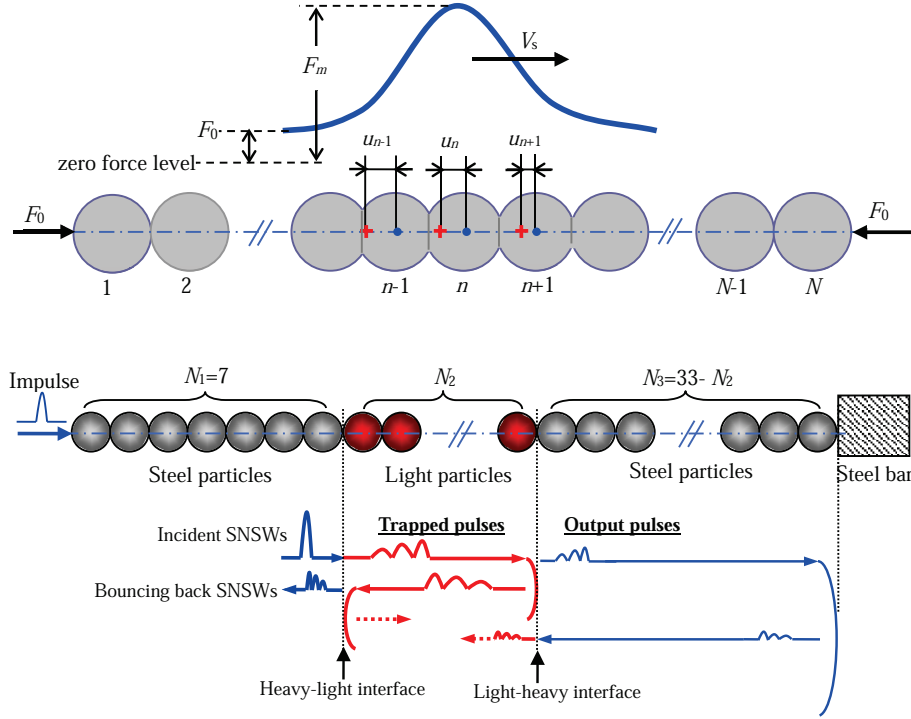


Figure 1. One-dimensional diagram of uniform granular chain (top) and composite granular chain for supporting strongly nonlinear solitary waves (bottom).

In a 1-D chain composed of identical spherical particles, the propagation velocity of SNSWs V_s can be expressed as a function of the ratio of static and the maximum dynamic force $f_r = F_m/F_0$, where F_m includes static precompression force F_0 [Nesterenko 2001]:

$$V_s = 0.9314 \left(\frac{4E^2 F_0}{a^2 \rho^3 (1-v^2)^2} \right)^{1/6} \frac{1}{(f_r^{2/3} - 1)} \left\{ \frac{4}{15} [3 + 2f_r^{5/3} - 5f_r^{2/3}] \right\}^{1/2}. \quad (3)$$

When the chain is uncompressed, equation (3) can be simplified as

$$V_s = 0.6802 \left(\frac{2E}{a\rho^{3/2}(1-v^2)} \right)^{1/3} F_d^{1/6}. \quad (4)$$

The maximum contact force F_m among the particles during the propagation of solitary waves remains constant in nondissipative systems [Nesterenko 2001]. In reality, energy dissipation is unavoidable. However, it is still difficult to accurately predict energy dissipation of SNSWs along its propagation due to the factors of contact plasticity, inelastic restitution of the particles, reflection at interface, and friction between the chain and its holder [Wang and Nesterenko 2015; Rosas and Lindenberg 2003; Rosas et al. 2008]. Therefore, in the subsequent finite element simulation, the propagation behavior of pulse waves in 1-D granular chain was only investigated for nondissipative systems. Energy attenuation of pulse waves along its propagation in the composite chain was evaluated by experimental tools.

In the case, the composite granular chain is composed of a total of 40 spherical particles which have the identical diameter of 10 mm and can be divided into three sections. Seven steel particles are placed in the first section of the chain (referred to heavy section) to generate a pulse close to steady strongly nonlinear solitary wave when impact force applied on the first particle is of significantly short duration or due to impact by striker with mass equal or less than mass of particles in the chain. The second section of the chain includes a certain amount (varying in the range of 3–24) of particles of lower Young's modulus and density (referred as light section) compared to steel particles. The third section of the chain (heavy section) is also composed of steel particles and its last particle directly contacts with a steel bar.

The propagation of the pulse waves along the composite granular chain is more complex than that in a chain composed of identical particles. It is already known that the incident SNSWs from the heavy sectional chain are transformed into an oscillatory pulse which on later stage is split into a sequence of strongly nonlinear solitary waves [Nesterenko et al. 1995; Daraio et al. 2006b; Sen et al. 2008]. Energy reflections do not occur unless pulse waves travel from the light section to the heavy section. As a result, the sequence of pulse waves propagating along the light section bounce back and forth between the light-heavy and heavy-light interfaces (Figure 1, bottom), as suggested by the reported interesting energy trapping behavior [Wang et al. 2007]. Due to the energy trapping effect, the peak amplitude of the output pulse waves transmitted into the third sectional chain is lower than that of the impact applied on the first sectional chain. Therefore, the composite granular chain can work as a protector to mitigate the strength of external impact applied on the steel bar.

For the composite granular chain shown in Figure 1 (bottom), the energy of pulse waves transmitted into the third section of the chain can be tunable by employing particles of different materials. To improve the performance of the protector, soft materials with a small Young's modulus and density are generally recommended for the light sectional chain. However, the effect of the length of the light section on the quantity of energy transmitted into the third section of the chain has not been reported yet. In addition, the reflection behavior of the trapped sequence of pulse waves at the light-heavy interface was also not experimentally observed or discussed.

3. Numerical modeling

3.1. Descriptions of the FE model. To simulate the propagation of pulse waves in the composite granular chain, inspired by the report in [Musson and Carlson 2014], finite element models were developed in COMSOL. The penalty function was employed to solve the contact problem among the particles in 1-D granular chain of spherical particles. First, a 1-D chain composed of identical elastic spherical particles was modeled to optimize the mesh size, penalty factor, and solver by comparing the simulated results with that predicted with (4). Second, a 1-D composite granular chain shown in Figure 1 (bottom) was modeled with the optimal numerical scheme to investigate the propagation characteristics of the trapped and output pulses.

Two-dimensional axial symmetry operation was applied in the model shown in Figure 2 (top left) to obtain a 1-D chain composed of fifteen stainless steel particles. The properties of the stainless steel are listed in Table 1. To save computational resources, the diameter of the particles was selected as 4.76 mm, which was smaller than that of the particles in the composite granular chain. The last particle at the

bottom of the chain contacted with a stainless steel cylinder, whose diameter and height were about 20 mm and 10 mm, respectively.

Starting from the contact point between two adjacent particles, the arc with the length of $\pi/18$ is defined as the contact boundary. A contact pair shown in Figure 2 (top right) consists of a *source* and *destination* contact boundary. The contact force was transferred from the *source* contact boundary to the *destination* contact boundary. The displacements of the centers of all the particles were fixed as zero in r direction to limit the rotation and translation. The fixed constraint was applied to the bottom surface of the cylinder and the remaining surfaces of the entire model had free boundaries.

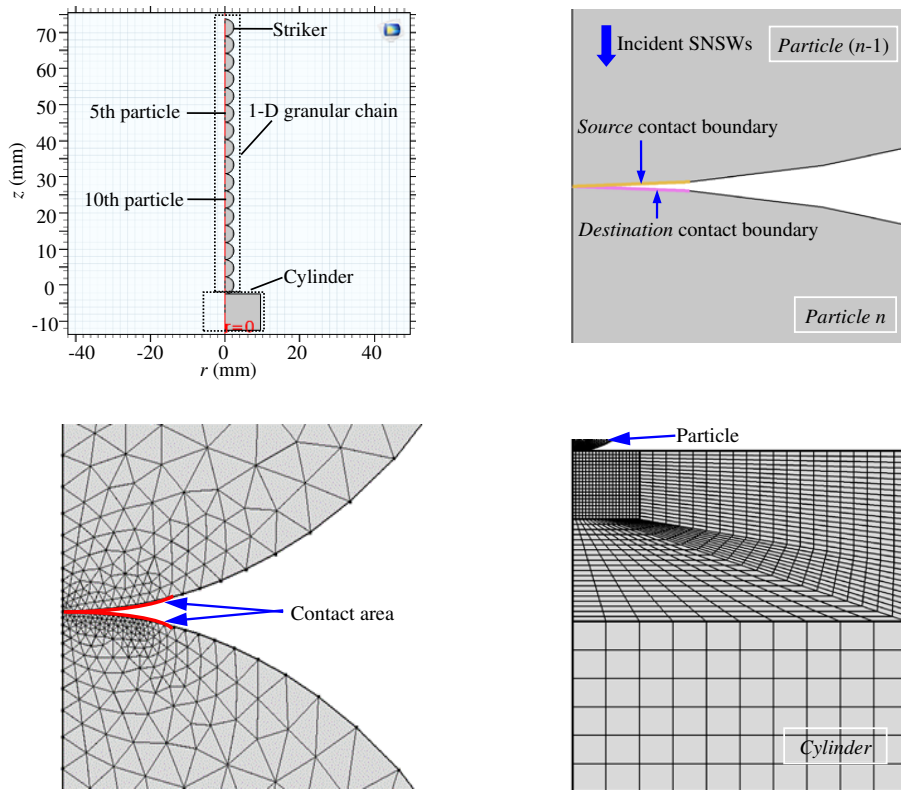


Figure 2. Finite element simulation model of 1-D granular chain. Top: geometrical configuration of the entire model (left) and the contact pair (right). Bottom: meshing results of the contact area between two adjacent particles (left) and between the last particle of the chain and the bottom cylinder (right).

materials	density (g/m^3)	Young's modulus (GPa)	Poisson's ratio
stainless steel	7925	209	0.28
Brass	8398	103	0.34
PTFE	1870	1.46	0.46

Table 1. Properties of granular materials.

The contact pair was discretized with free three-noded elements and then the particles were meshed with free triangular nodes by the automatic generation algorithm. To achieve the more accurate solution, the *destination* contact boundary employed the finer mesh than that of the *source* contact boundary after repeated trials. The meshing operation of the cylinder was performed according to the procedures recommended by the case of *Cylinder Roller Contact* in COMSOL. In the cylinder, the mesh size near the contact area between the particle and the top surface of the cylinder was much smaller than that of the region far away from the contact area.

The top stainless steel particle of the chain acted as a striker with an initial speed of 0.626 m/s and then the propagation of SNSWs in the chain was simulated in the finite element models established above. The mesh size and the penalty factor, which determined the performance of the penalty function on solving the contact problem, were optimized with the single factor analysis method. The relative errors between the simulated velocities of the SNSWs and the results predicted by the Hertzian contact theory were used as a criterion for evaluating the effects of the mesh size and penalty factor on the computation accuracy of the FE model.

3.2. Parameter optimization.

3.2.1. Mesh size. The penalty factor was fixed as a constant with a value of $\eta = 1$ and *constant* solver was employed to give the solutions of the solitary wave propagation. The profile of the contact force at the interaction zone between two adjacent particles was extracted from the simulation results when the minimal mesh size (β) of the model was gradually reduced from 0.2 mm to 0.01 mm.

The contact force profiles corresponding to the contact pair of the 5th and 6th particles and the contact pair of the tenth and eleventh particles are plotted in Figure 3. The time interval between the two peaks of the contact force profiles is divided by the distance of five-time diameters of the particle to estimate the propagation velocity (V_{sw}) of the solitary wave.

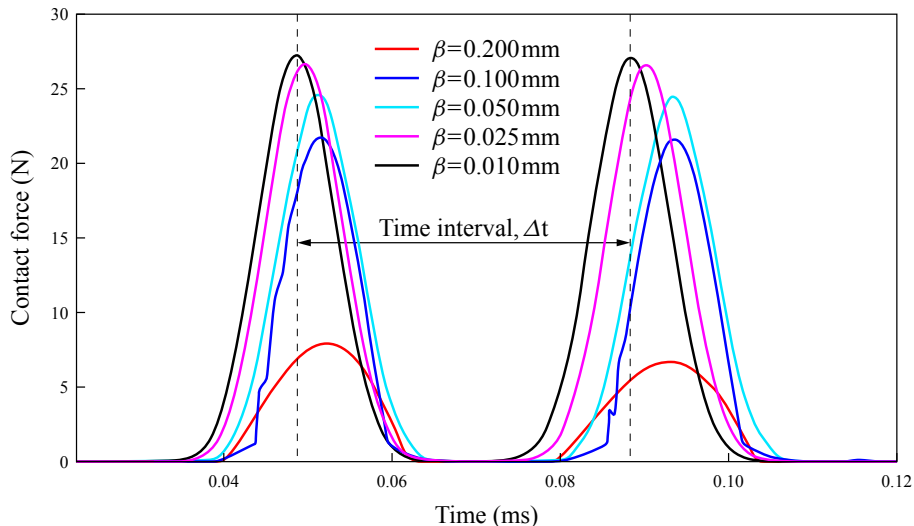


Figure 3. Profiles of contact force obtained from the model with different mesh sizes.

model no.	mesh size (mm)	contact force (N)	velocity of SNSWs		time consumption
			value (m/s)	error (%)	
1	0.2–0.4	7.92	590	20.00	9 min 24 s
2	0.1–0.2	21.71	569	2.14	18 min 49 s
3	0.05–0.1	24.55	566	4.63	31 min 16 s
4	0.025–0.05	26.62	586	2.58	1 h 9 min
5	0.01–0.02	27.17	599	0.76	3 h 21 min 3 s

Table 2. Performances of the models with different mesh sizes.

As indicated in (4), for the granular chain of a given material, the velocity of the SNSWs is proportional to the value of $F_m^{1/6}$. When the minimal mesh size of 0.2 mm was selected in the model, the obtained maximum contact force was significantly lower than that of other cases and a relative error between the simulated value of V_{sw} and the theoretical velocity of SNSWs was 20.00%. When the minimal mesh size decreased from 0.2 mm to 0.1 mm, the maximum contact force in the simulation substantially increased from 7.92 N to 21.71 N and the obtained relative error of the velocity was decreased to 2.14%. However, the profile of the contact force was not smooth especially in the initial stage of the contact, indicating that the model could not achieve the high-precision simulation of the propagation of SNSWs.

Therefore, the model utilizing the smaller mesh size was further investigated. When the minimal mesh size was alternatively selected as 0.05 mm, 0.025 mm, and 0.01 mm, the calculation error of velocity and simulation time are summarized in Table 2. The FE models are solved by the COMSOL software which is run in a computer with two processors of Intel Xeon X5650 (RAM: 64 GB, main frequency: 2.66 GHz). In the simulation cases, the minimal calculation error of 0.67% could be realized after the longest simulation time with the smallest mesh size of 0.01 mm (Case 5). To balance the calculation error and simulation time, the minimal mesh size was selected as 0.025 mm in the subsequent simulation even though the calculation error was slightly higher than that in Case 5. The total number of degree of freedom in the selected model solution is 115634.

3.2.2. Penalty factor and solver. For the purpose of solving some optimization problems, an additional function (penalty function) should be added to the original objective function in order to obtain an augmented objective function [Greenberg and Pierskalla 1970]. The penalty function is generally used to transform the constrained optimization problem into an unconstrained optimization problem [Bellmore et al. 1970; Hinch and Saint-Jean 1999]. The penalty factor η is an important parameter of the penalty function.

The similar simulation procedure as previously discussed is used to investigate the effect of penalty factor η in the penalty function on the calculation error of velocity. When the value of η gradually increases from 1.1 to 1.5 with a step of 0.1, the high-quality contact force profiles can be obtained with the *Constant* solver. The simulated values of F_m and velocities are listed in Table 3. The relative error of velocity continuously decreases from 2.47% to 1.57% as the penalty factor increases from 1.1 to 1.4. As for the case of $\eta = 1.5$, the simulation results show that the maximum contact force further increases compared to the case of $\eta = 1.4$, thus leading to an increase in propagation velocity according to (4). Surprisingly, the velocity estimated from the simulation results is about 590 m/s (Table 3), which

penalty factor, η	contact force, F (N)	velocity of solitary wave, V_{sw}	
		values (m/s)	errors (%)
1.1	26.71	587	2.47
1.2	26.77	590	2.01
1.3	26.81	592	1.70
1.4	26.86	592	1.57
1.5 (constant solver)	27.36	590	2.36
1.5 (automatic solver)	27.22	595	0.40

Table 3. Results obtained from the model with different penalty factors and solvers.

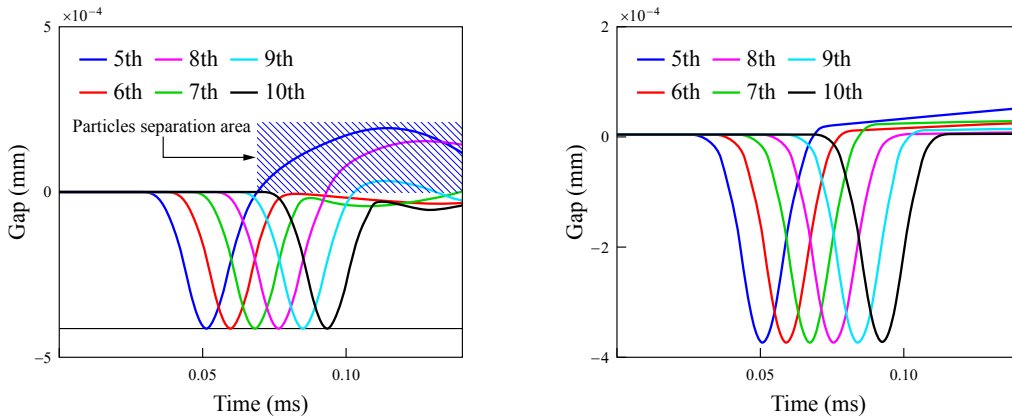


Figure 4. Gap between two adjacent particles obtained from the model with constant solver (left) and automatic solver (right).

is slower than that obtained in the case of $\eta = 1.4$. As shown in Figure 4, the value of the gap at the contact point between the 5th and 6th particles remains to be negative due to the compression before the time of 0.6 ms. Then it has the positive sign, indicating that the separation phenomenon of particles occurs during the propagation of SNSWs. The similar behavior can also be observed from the results extracted at the 10th contact pair. The separation phenomenon of the particles may induce the second impact among the particles [Wang and Nesterenko 2015; Rosas et al. 2008].

To solve the problem of the *Constant* solver, the *Automatic* solver was adopted to provide more convincing results (Figure 4, right). Although slight separation could be concluded from the profile of gap versus time, the velocity calculation error significantly decreased to 0.4% (Table 3).

With the optimal parameters of mesh size ($\beta = 0.025$ mm) and penalty factor ($\eta = 1.5$), the solutions of the model provided by *Automatic* solver were used to explore the relationship between the contact force and the relative displacement between the centers of the 5th and 6th particles. The results in Figure 5 demonstrated that the dependency of the dynamic contact force on the relative displacement yielded a power function with an exponent of 1.554, which was close to the value of 1.5 suggested by the Hertzian contact law [Hertz 1881]. The results in Figure 5 and Table 3 proved that the finite element model with

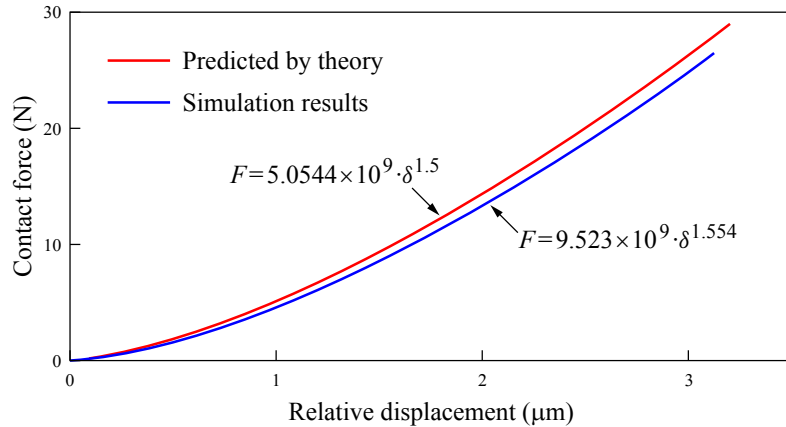


Figure 5. Comparison between the predicted and simulated results of the dependency of contact force on the relative displacement.

optimal parameters and solver could be applied to accurately simulate the propagation of SNSWs in 1-D granular chain of spheres.

3.3. Propagation behaviors of pulse waves in composite chain. The finite element model together with its optimal parameters (mesh size, penalty factor, and solver) obtained in Section 3.2 was used to investigate the propagation of SNSWs in a 1-D composite granular chain of spheres (Figure 1, bottom). In the simulation model, the material of the spherical particles in the light sectional chain was alternatively selected as Brass and PTFE, whose properties are listed in Table 1.

The initial speed of the striker particle was fixed at 0.626 m/s in all the simulation models. Due to the energy trapping effect governed by the light-heavy and heavy-light interfaces, the propagation behaviors of pulse waves in the light chain was complicated. So far, the multiple reflection behavior of the pulse waves in the light chain was seldom explored with simulation tools. Here, as an example, the simulation results obtained from the model with $N_2 = 6$ particles in the light section were extracted to observe the reflection behavior of output pulse waves in the composite chain. The profile of contact force versus time shown in Figure 6 was extracted from the contact pair formed with the third and fourth particles in the light section.

In the model with light sectional chain of Brass, one round of back and forth reflections can be identified in the profile shown in Figure 6 (left). The pulse waves reflected from the light-heavy interface are in the form of a single impulse, which is referred to back reflection wave (BRW). When the BRW returns to the heavy-light interface, partial energy of BRW will be reflected again to generate the forth reflection wave (FRW). When the original incident pulse wave passes through the heavy-light interface, as suggested in the previous study [Hong and Xu 2002], partial energy of the pulse waves is stored in the particles in the form of compressive deformation. The BRW imposes propulsive force onto the contact area at the heavy-light interface and consequently deformation recovery happens, thus leading to additional impact on the light section and generating a delayed forth reflection wave (DFRW) (Figure 6, left).

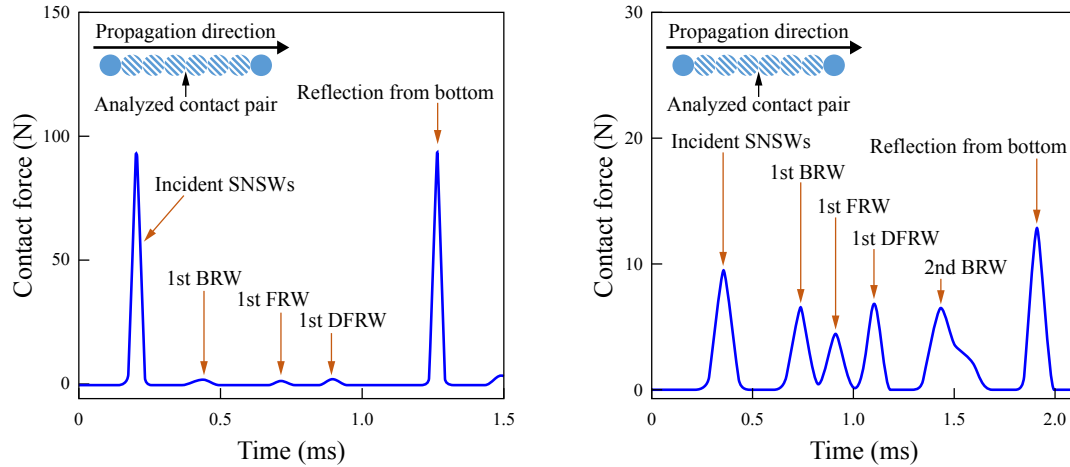


Figure 6. Profiles of contact force extracted at the analyzed contact pair in the model of composite chain with the light sectional chain of Brass (left) and PTFE (right).

Similar reflection behavior of pulse waves at the first round of back and forth reflections can be observed in the case with the light chain of PTFE. As sketched in Figure 6 (right), two reflected wave packets are respectively generated by the mechanism of interface reflection and the deformation recovery and can be identified during the process of the first forth reflection of pulse waves. The contact stiffness between PTFE particle and steel particle was much lower than that between Brass particle and steel particle. As emphasized in the previous report [Daraio et al. 2006b], for the fixed incident pulse waves, the amount of energy reflected at the contact pair with low contact stiffness was higher than that in the case of high contact stiffness. Accordingly, in the case with the light chain of PTFE, the ratio of energy of BRW to the output pulses transmitted through the light-heavy interface was much higher than that in the case with the light chain of Brass. In other words, a larger amount of energy of pulse waves was trapped inside the light chain of PTFE compared to that in the light chain of Brass.

In the third section of the composite chain, the propagation velocity of pulse waves was determined by the peak contact force at the contact pair [Rosas and Lindenberg 2003]. In the composite chain with the light chain of PTFE, the amount of energy (or peak contact force) transmitted into the third section chain was much smaller than that in the case with light chain of Brass. Thus, the output pulses of the composite chain propagated more slowly in the case with the light chain of PTFE than that in the case of Brass chain. The propagation time of the pulse waves reflected from the bottom cylinder was around 1.85 ms, which was longer than the propagation time of 1.25 ms estimated from Figure 6 (left). The delay of pulse waves reflected from the bottom cylinder allowed the longer time window to observe the reflection behavior of pulse waves in the light section and the second back reflection wave could also be captured (Figure 6, right).

To carefully investigate the energy transmission efficiency (λ) of pulse waves at the light-heavy interface, the profiles of contact force were extracted at the second contact pair in the third sectional chain. With the increase in the number of light particles, the results of the contact force profiles for the cases with the light chains of Brass and PTFE are plotted in Figure 7 (left and right, respectively). The amount

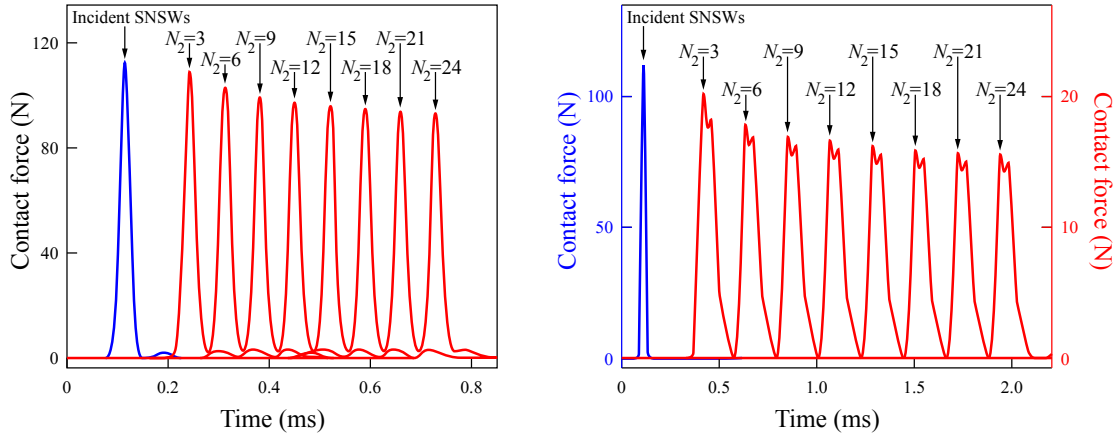


Figure 7. Effects of the number of light particles on the transmitted pulse waves in the model of composite chain with the light section of Brass (left) and PTFE (right).

of the energy of incident pulse waves was fixed due to the constant impact condition imposed on the composite chain. Hence, the effect of the length of light section on the energy transmission efficiency λ could be evaluated by verifying the results in Figure 7.

For both cases of the composite chain, the peak contact force of the transmitted (or output) pulses demonstrated the exponentially decreasing trend with the increase in the value of N_2 . During the propagation of the pulse waves in the first chain, the total energy density of the pulse waves (including the elastic energy and kinematic energy) retains as constant (see Figure 8). This confirmed that the energy dissipation caused by material attenuation and friction is not considered in the simulation model.

However, the total energy of the pulse waves in the light section chain demonstrates successive attenuation as the propagation of the pulse waves (see Figure 8). The maximum compressive stress in the contact area of Brass sphere is changed from 1200 MPa to 1110 MPa, and for the PTFE sphere is changed from 35 MPa to 20 MPa. The Young's modulus of the light spheres is much lower than that of the steel spheres used in the first chain. As a result, the maximum compressive stress in the contact area of two light spheres may exceed the yield strength of the material of Brass and PTFE. Therefore, plastic

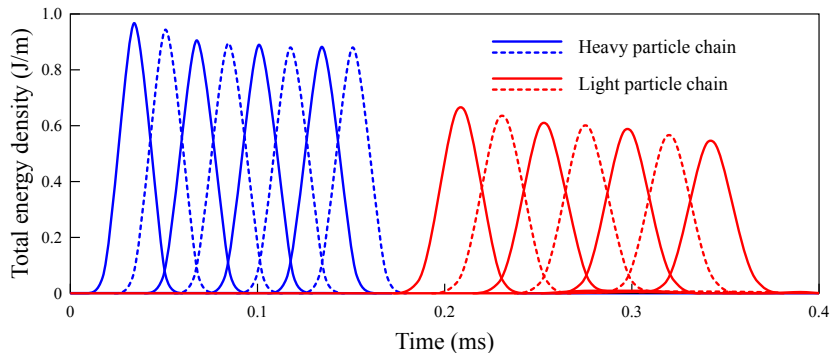


Figure 8. The total energy density of the heavy particles and light particles.

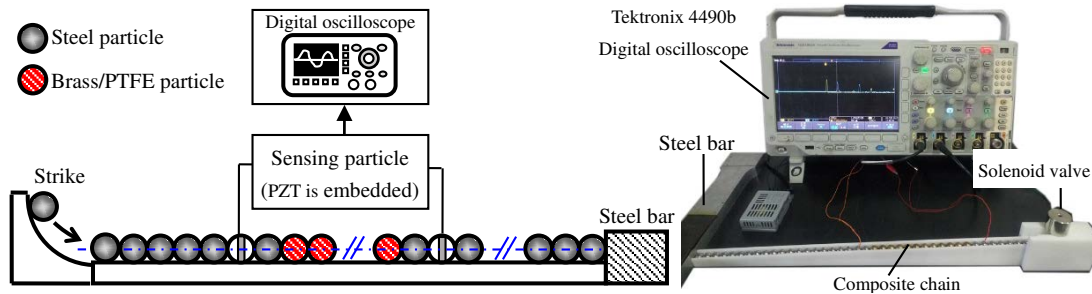


Figure 9. Schematic diagram (left) and photo of the experimental setup (right).

deformation occurs at the contact area of two light spheres and part of the pulse waves' energy is stored in the form of plastic deformation. The decay of the output energy of pulses was attributed to plastic deformation when pulse waves passed through the light section [Musson and Carlson 2014; 2016].

The profile of the contact force extracted from the case of PTFE showed two peaks. We believed that the collision between the incident pulse waves and the BRW induced secondary collisions at the light-heavy interface. The time interval between the two collisions was short and the output pulses were overlapped to exhibit the double-peak character. The double-peak character in the waveform of transmitted pulse waves was confirmed by subsequent experimental results. The decay of energy transmission efficiency is quantitatively analyzed in Section 4.

4. Experimental verification and discussion

Experimental observation of the propagation behavior of pulse waves was conducted in a one-dimensional composite granular chain composed of 40 spherical particles (see in Figure 9). The diameter of all the particles was identical to that used in the simulation model. The configuration of the composite chain was also identical to that illustrated in Figure 1 (bottom). Two sensing particles were respectively used to replace the sixth particle in the first sectional chain and the second particle in the third sectional chain to sense the propagation of pulse waves. Each sensing particle was made by cutting a steel particle into halves and embedding a PZT wafer between the two halves [Daraio et al. 2006a; 2006b]. The sandwich structure of the sensing particle was boned with epoxy and the voltage signals output by the PZT wafer was acquired by a Tektronix 4490b digital oscilloscope with a sampling frequency of 10 MHz.

The well-arranged composite chain was placed in a plastic holder with an inclination angle of 3° in order to achieve the intact contact between every two adjacent particles [Leonard et al. 2014]. A solenoid valve was used to hold and release the steel striker particle with a diameter of 10 mm. The distance between the center of striker and the center of the first particle in the chain was adjusted to be around 20 mm and the estimated speed of the impact imposed on the composite chain was about 0.626 m/s.

The light chain was alternatively fulfilled with the particles of Brass and PTFE. Figure 10 shows the signal of pulse waves measured by the two sensing particles in the experimental tests. As predicted with the simulation results in Figure 7, in the two cases, the peak voltage induced by the propagation of pulse waves demonstrated the exponential attenuation behavior with the increase in the propagation distance.

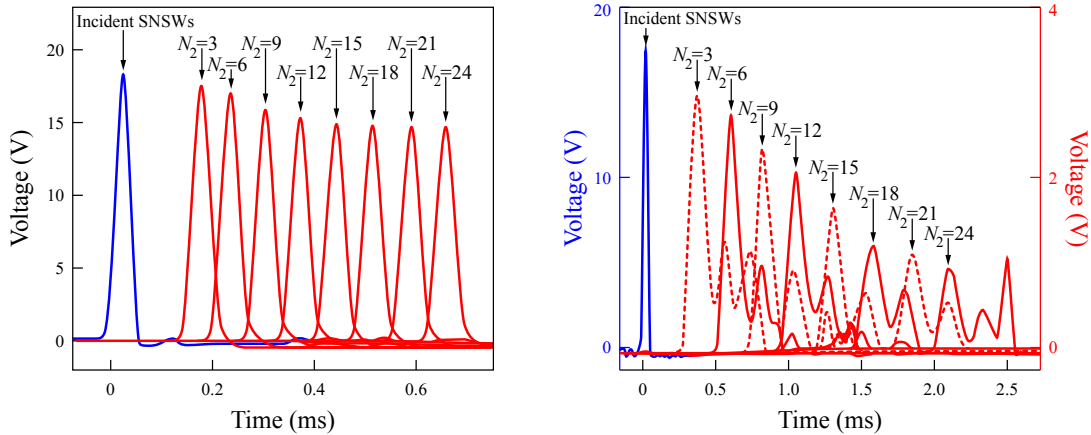


Figure 10. Effects of the number of light particles on the transmitted pulse waves in the experiment of composite chain with the light section of Brass (left) and PTFE (right).

The ratio of the peak amplitude of incident pulse waves to the peak amplitude of output pulses was treated as the energy transmission efficiency (λ). In addition, the time interval (Δt) between the peak voltages of the incident and transmitted pulse waves were estimated. The propagation distance (L) was divided by the time interval (Δt) to estimate the propagation velocity (V_{sw}) of the pulse waves. The estimated results of λ and V_{sw} are plotted in Figure 11.

Experimental results were compared with simulation results based on the results shown in Figure 11. For the composite chain with the light section of Brass, the measured propagation velocity of pulse waves exponentially decayed from the initial value of 469 m/s ($N_2 = 3$) to around 424 m/s ($N_2 = 24$). The measured value of V_{sw} was lower than the predicted value and the error might come from the mismatch of material properties between the true particle and the particle in the simulation model. Among the investigated cases, the maximum relative error between the simulated propagation velocity and measured propagation velocity was about 4.2%. In the case with the light chain of PTFE, the curve fitted to the predicted data was close to that fitted to the measured data (Figure 11, right). In the initial stage ($N_2 = 1$), the prediction error of propagation velocity was about 17.1%. When the value of N_2 was larger than 3, the prediction error dramatically decreased below 2.3%, indicating that the previously established finite element models possessed the good prediction performance in the propagation velocity of the pulse waves in the investigated composite chain.

In the studied two cases of the composite chain, both the measured and predicted results of energy transmission efficiency showed the exponential decay trend. Hence, the light sectional chain had the effects of velocity reduction and amplitude attenuation on the input pulse waves transmitted from the first sectional chain. The propagation velocity and the amplitude of the output pulses were determined by both the material properties and the number of light particles in the simulation results. Erenow, the phenomenon similar to that demonstrated in Figure 11, was only reported at the nanoscale in simulation studies. The results in Figure 11 indicated that even at the macroscale the investigated composite chain was able to quantitatively tune the amplitude and propagation velocity of pulse waves by adjusting the number of particles in the light sectional chain.

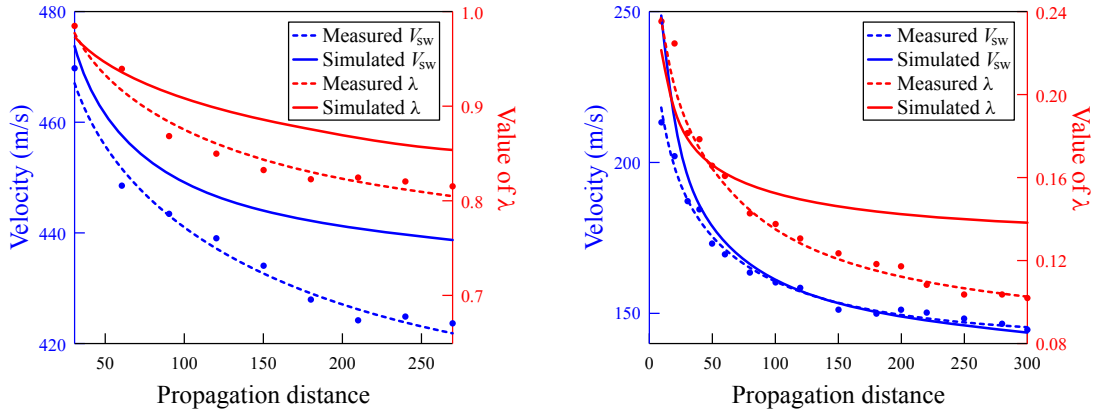


Figure 11. Amplitude and velocity obtained by the experiment and simulation for the particles with the low elastic modulus: Brass particles (left) and PTFE particles (right).

At the initial stage ($N_2 = 3$), the prediction error of the value of λ was as small as 0.53% for the case with the light chain of Brass and a prediction error was 1.3% for the case with the light chain of PTFE. When the number of Brass (or PTFE) particles was larger than 6, the difference between the measured energy transmission efficiency and the predicted energy transmission efficiency increased with the increase in the propagation distance. In the experiment, along with the propagation of pulse waves in the light chain, the inevitable friction between the particles and the plastic holder caused additional energy dissipation to pulse waves. The longer propagation distance corresponded to the more dissipated energy. The accumulation effect of the energy dissipation led to the continuously increasing error between the measured and predicted values of λ .

The light sectional chain can act as a physical regulator to control the properties of the output pulse waves. When the number of light particles was fixed, compared to the light Brass chain, the light PTFE chain caused the more serious attenuation on the amplitude of the pulse waves and more significantly decreased the propagation velocity of the output pulse waves. When the material of the light particle was selected, the dependency of both the propagation velocity and the amplitude of the output pulse waves on the number of light particle could be predicted with the proposed finite element simulation model. However, the predicted values of V_{sw} and λ were larger than corresponding actual results because the mechanical frictions in the system of composite chain were not considered in the simulation model.

5. Conclusion

The propagation characteristics of the trapped and output strongly nonlinear solitary waves in 1-D composite granular chain of spherical particles were explored in this study. Finite element simulation was performed with optimal mesh size, penalty factor, and solver and the obtained results confirmed that the energy tunnel behavior, which had been reported at the nanoscale [Xu and Zheng 2017], was also applicable to the composite chain at the macroscale. More precisely, the propagation velocity and the amplitude of the finally output pulse waves in the composite chain could be tuned by adjusting the material and the number of light particles.

Though the energy dissipation caused by viscoplastic deformation of particles or friction was not considered in the simulation model, the total energy of the pulse waves in the light section chain successively decays as the propagation of the pulse waves. This is because plastic deformation occurs at the contact area of two light spheres and part of the pulse waves' energy is stored in the form of plastic deformation. As a result, the propagation velocity and the amplitude of the output pulse waves could be exponentially reduced by increasing the number of light particles.

Verification experiments were performed to confirm the conclusions obtained from simulations. However, in the experiments unavoidable energy dissipation of SNSWs along its propagation occurs due to viscoplastic deformation of particles and friction. Thus the finite element simulation results has a systemic overestimation in predicting the propagation velocity and the amplitude of the output pulse waves. However, the established finite element simulation model could be used to investigate the multireflection behavior of the output pulse waves and reveal the effects of the configuration and material of the light sectional chain on the properties of the output pulse waves.

Acknowledgements

This study was supported by the National Natural Science Foundation of China (Project No. 11572011) and the International Research Cooperation Seed Fund of Beijing University of Technology (Project No. 2018A07).

References

- [Bellmore et al. 1970] M. Bellmore, H. J. Greenberg, and J. J. Jarvis, "Generalized penalty-function concepts in mathematical optimization", *Oper. Res.* **18**:2 (1970), 229–252.
- [Brogliato 2016] B. Brogliato, *Nonsmooth mechanics: models, dynamics and control*, Springer, London, 2016.
- [Carretero-González et al. 2009] R. Carretero-González, D. Khatri, M. A. Porter, P. G. Kevrekidis, and C. Daraio, "Dissipative solitary waves in granular crystals", *Phys. Rev. Lett.* **102**:2 (2009), 024102.
- [Daraio et al. 2006a] C. Daraio, V. F. Nesterenko, E. B. Herbold, and S. Jin, "Tunability of solitary wave properties in one-dimensional strongly nonlinear phononic crystals", *Phys. Rev. E* **73**:2 (2006), 026610.
- [Daraio et al. 2006b] C. Daraio, V. F. Nesterenko, E. B. Herbold, and S. Jin, "Energy trapping and shock disintegration in a composite granular medium", *Phys. Rev. Lett.* **96**:5 (2006), 058002.
- [Falcon et al. 1998] E. Falcon, C. Laroche, S. Fauve, and C. Coste, "Collision of a 1-D column of beads with a wall", *Eur. Phys. J. B* **5**:1 (1998), 111–131.
- [Gantzounis et al. 2013] G. Gantzounis, M. Serra-Garcia, K. Homma, J. M. Mendoza, and C. Daraio, "Granular metamaterials for vibration mitigation", *J. Appl. Phys.* **114**:9 (2013), 093514.
- [Greenberg and Pierskalla 1970] H. J. Greenberg and W. P. Pierskalla, "Surrogate mathematical programming", *Oper. Res.* **18**:5 (1970), 924–939.
- [Hertz 1881] H. Hertz, "On the contact of elastic solids", *J. Reine Angew. Math.* **92** (1881), 156–171.
- [Hinch and Saint-Jean 1999] E. J. Hinch and S. Saint-Jean, "The fragmentation of a line of balls by an impact", *Proc. R. Soc. Lond. A* **455**:1989 (1999), 3201–3220.
- [Hong 2005] J. Hong, "Universal power-law decay of the impulse energy in granular protectors", *Phys. Rev. Lett.* **94**:10 (2005), 108001.
- [Hong and Xu 2002] J. Hong and A. Xu, "Nondestructive identification of impurities in granular medium", *Appl. Phys. Lett.* **81**:25 (2002), 4868–4870.
- [Khatri 2012] D. Khatri, *Non-destructive evaluation of material system using highly nonlinear acoustic waves*, Ph.D. thesis, California Institute of Technology, 2012, Available at <https://thesis.library.caltech.edu/7022/>.

- [Khatri et al. 2012] D. Khatri, D. Ngo, and C. Daraio, “Highly nonlinear solitary waves in chains of cylindrical particles”, *Granul. Matter* **14**:1 (2012), 63–69.
- [Kim et al. 2015] E. Kim, R. Chaunsali, H. Xu, J. Jaworski, J. Yang, P. G. Kevrekidis, and A. F. Vakakis, “Nonlinear low-to-high-frequency energy cascades in diatomic granular crystals”, *Phys. Rev. E* **92**:6 (2015), 062201. also in arXiv:1505.05556v2.
- [Kim et al. 2017] E. Kim, J. Yang, H.-Y. Hwang, and C. W. Shul, “Impact and blast mitigation using locally resonant woodpile metamaterials”, *Int. J. Impact Eng.* **101** (2017), 24–31.
- [Kuninaka and Hayakawa 2009] H. Kuninaka and H. Hayakawa, “Simulation of cohesive head-on collisions of thermally activated nanoclusters”, *Phys. Rev. E* **79**:3 (2009), 031309. also in arXiv:0812.5035v2.
- [Leonard et al. 2014] A. Leonard, C. Chong, P. G. Kevrekidis, and C. Daraio, “Traveling waves in 2D hexagonal granular crystal lattices”, *Granul. Matter* **16**:4 (2014), 531–542. also in arXiv:1305.0171v1.
- [Li and Rizzo 2015a] K. Li and P. Rizzo, “Energy harvesting using an array of granules”, *J. Vib. Acoust. (ASME)* **137**:4 (2015), 041002.
- [Li and Rizzo 2015b] K. Li and P. Rizzo, “Energy harvesting using arrays of granular chains and solid rods”, *J. Appl. Phys.* **117**:21 (2015), 215101.
- [Meidani et al. 2015] M. Meidani, E. Kim, F. Li, J. Yang, and D. Ngo, “Tunable evolutions of wave modes and bandgaps in quasi-1D cylindrical phononic crystals”, *J. Sound Vib.* **334** (2015), 270–281.
- [Musson and Carlson 2014] R. W. Musson and W. Carlson, “Simulation of solitary waves in a monodisperse granular chain using COMSOL multiphysics: localized plastic deformation as a dissipation mechanism”, *Granul. Matter* **16**:4 (2014), 543–550.
- [Musson and Carlson 2016] R. W. Musson and W. Carlson, “Plastic deformation in a metallic granular chain”, *Comput. Part. Mech.* **3**:1 (2016), 69–82.
- [Nesterenko 1983] V. F. Nesterenko, “Propagation of nonlinear compression pulses in granular media”, *J. Appl. Mech. Tech. Phys.* **24**:5 (1983), 733–743.
- [Nesterenko 2001] V. F. Nesterenko, *Dynamics of heterogeneous materials*, Springer-Verlag, New York, 2001.
- [Nesterenko et al. 1995] V. F. Nesterenko, A. N. Lazaridi, and E. B. Sibiriyakov, “The decay of soliton at the contact of two “acoustic vacuums””, *J. Appl. Mech. Tech. Phys.* **36**:2 (1995), 166–168.
- [Nesterenko et al. 2005] V. F. Nesterenko, C. Daraio, E. B. Herbold, and S. Jin, “Anomalous wave reflection at the interface of two strongly nonlinear granular media”, *Phys. Rev. Lett.* **95**:15 (2005), 158702.
- [Ngo et al. 2011] D. Ngo, D. Khatri, and C. Daraio, “Highly nonlinear solitary waves in chains of ellipsoidal particles”, *Phys. Rev. E* **84**:2 (2011), 026610.
- [Ngo et al. 2013] D. Ngo, S. Griffiths, D. Khatri, and C. Daraio, “Highly nonlinear solitary waves in chains of hollow spherical particles”, *Granul. Matter* **15**:2 (2013), 149–155.
- [Nguyen and Brogliato 2014] N. S. Nguyen and B. Brogliato, *Multiple impacts in dissipative granular chains*, Springer, Berlin, 2014.
- [Potekin et al. 2013] R. Potekin, K. R. Jayaprakash, D. M. McFarland, K. Remick, L. A. Bergman, and A. F. Vakakis, “Experimental study of strongly nonlinear resonances and anti-resonances in granular dimer chains”, *Exp. Mech.* **53**:5 (2013), 861–870.
- [Przedborski et al. 2015] M. A. Przedborski, T. A. Harroun, and S. Sen, “Localizing energy in granular materials”, *Appl. Phys. Lett.* **107**:24 (2015), 244105. also in arXiv:1601.02656v1.
- [Raney et al. 2016] J. R. Raney, N. Nadkarni, C. Daraio, D. M. Kochmann, J. A. Lewis, and K. Bertoldi, “Stable propagation of mechanical signals in soft media using stored elastic energy”, *Proc. Nat. Acad. Sci. USA* **113**:35 (2016), 9722–9727.
- [Rizzo and Li 2017] P. Rizzo and K. Li, “Analysis of the geometric parameters of a solitary waves-based harvester to enhance its power output”, *Smart Mater. Struct.* **26** (2017), 075004.
- [Rizzo et al. 2015] P. Rizzo, A. Bagheri, and E. La Malfa Ribolla, “Highly nonlinear solitary waves for the NDT of slender beams”, pp. 173–177 in *Emerging Technologies in Non-Destructive Testing VI: Proceedings of the 6th International Conference on Emerging Technologies in Nondestructive Testing* (Brussels), 2015.

- [Rosas and Lindenberg 2003] A. Rosas and K. Lindenberg, “Pulse dynamics in a chain of granules with friction”, *Phys. Rev. E* **68**:4 (2003), 041304. also in arXiv:cond-mat/0307080v1.
- [Rosas et al. 2008] A. Rosas, A. H. Romero, V. F. Nesterenko, and K. Lindenberg, “Short-pulse dynamics in strongly nonlinear dissipative granular chains”, *Phys. Rev. E* **78**:5 (2008), 051303.
- [Sen et al. 2008] S. Sen, J. Hong, J. Bang, E. Avalos, and R. Doney, “Solitary waves in the granular chain”, *Phys. Rep.* **426**:2 (2008), 21–66.
- [Spadoni and Daraio 2010] A. Spadoni and C. Daraio, “Generation and control of sound bullets with a nonlinear acoustic lens”, *Proc. Nat. Acad. Sci. USA* **107**:16 (2010), 7230–7234.
- [Takato et al. 2018] Y. Takato, M. E. Benson, and S. Sen, “Small nanoparticles, surface geometry and contact forces”, *Proc. R. Soc. A* **474**:2211 (2018), 20170723.
- [Vergara 2005] L. Vergara, “Scattering of solitary waves from interfaces in granular media”, *Phys. Rev. Lett.* **95**:10 (2005), 108002.
- [Wang and Nesterenko 2015] S. Y. Wang and V. F. Nesterenko, “Attenuation of short strongly nonlinear stress pulses in dissipative granular chains”, *Phys. Rev. E* **91**:6 (2015), 062211.
- [Wang et al. 2007] P. J. Wang, J. H. Xia, Y. D. Li, and C. S. Liu, “Crossover in the power-law behavior of confined energy in a composite granular chain”, *Phys. Rev. E* **76**:4 (2007), 041305.
- [Xu and Nesterenko 2017] Y. Xu and V. F. Nesterenko, “Strongly nonlinear stress waves in dissipative metamaterials”, *AIP Conf. Proc.* **1793**:1 (2017), 120005.
- [Xu and Zheng 2017] J. Xu and B. Zheng, “Quantitative tuning nanoscale solitary waves”, *Carbon* **111** (2017), 62–66.
- [Zhao et al. 2008] Z. Zhao, C. Liu, and B. Brogliato, “Energy dissipation and dispersion effects in granular media”, *Phys. Rev. E* **78**:3 (2008), 031307.

Received 24 Jan 2019. Revised 1 Aug 2019. Accepted 7 Aug 2019.

BIN WU: wb@bjut.edu.cn

College of Mechanical Engineering and Applied Electronics Technology, Beijing University of Technology, Chaoyang District, 100 Pingleyuan Village, Beijing 100124, China

HEYING WANG: whyne2015@emails.bjut.edu.cn

College of Mechanical Engineering and Applied Electronics Technology, Beijing University of Technology, Chaoyang District, 100 Pingleyuan Village, Beijing 100124, China

XIUCHENG LIU: xiuchliu@bjut.edu.cn

College of Mechanical Engineering and Applied Electronics Technology, Beijing University of Technology, Chaoyang District, 100 Pingleyuan Village, Beijing 100124, China

MINGZHI LI: lmz1001@emails.bjut.edu.cn

College of Mechanical Engineering and Applied Electronics Technology, Beijing University of Technology, Chaoyang District, 100 Pingleyuan Village, Beijing 100124, China

ZONGFA LIU: lzf@haust.edu.cn

College of Civil Engineering, Henan University of Science and Technology, Luolong District, 263 Kaiyuan Avenue, Luoyang 471023, China

CUNFU HE: hecunfu@bjut.edu.cn

College of Mechanical Engineering and Applied Electronics Technology, Beijing University of Technology, Chaoyang District, 100 Pingleyuan Village, Beijing 100124, China

JOURNAL OF MECHANICS OF MATERIALS AND STRUCTURES

msp.org/jomms

Founded by Charles R. Steele and Marie-Louise Steele

EDITORIAL BOARD

ADAIR R. AGUIAR	University of São Paulo at São Carlos, Brazil
KATIA BERTOLDI	Harvard University, USA
DAVIDE BIGONI	University of Trento, Italy
MAENGHYO CHO	Seoul National University, Korea
HUILING DUAN	Beijing University
YIBIN FU	Keele University, UK
IWONA JASIUK	University of Illinois at Urbana-Champaign, USA
DENNIS KOCHMANN	ETH Zurich
MITSUTOSHI KURODA	Yamagata University, Japan
CHEE W. LIM	City University of Hong Kong
ZISHUN LIU	Xi'an Jiaotong University, China
THOMAS J. PENCE	Michigan State University, USA
GIANNI ROYER-CARFAGNI	Università degli studi di Parma, Italy
DAVID STEIGMANN	University of California at Berkeley, USA
PAUL STEINMANN	Friedrich-Alexander-Universität Erlangen-Nürnberg, Germany
KENJIRO TERADA	Tohoku University, Japan

ADVISORY BOARD

J. P. CARTER	University of Sydney, Australia
D. H. HODGES	Georgia Institute of Technology, USA
J. HUTCHINSON	Harvard University, USA
D. PAMPLONA	Universidade Católica do Rio de Janeiro, Brazil
M. B. RUBIN	Technion, Haifa, Israel

PRODUCTION production@msp.org

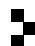
SILVIO LEVY Scientific Editor

See msp.org/jomms for submission guidelines.

JoMMS (ISSN 1559-3959) at Mathematical Sciences Publishers, 798 Evans Hall #6840, c/o University of California, Berkeley, CA 94720-3840, is published in 10 issues a year. The subscription price for 2019 is US \$635/year for the electronic version, and \$795/year (+\$60, if shipping outside the US) for print and electronic. Subscriptions, requests for back issues, and changes of address should be sent to MSP.

JoMMS peer-review and production is managed by EditFLOW[®] from Mathematical Sciences Publishers.

PUBLISHED BY

 **mathematical sciences publishers**
nonprofit scientific publishing

<http://msp.org/>

© 2019 Mathematical Sciences Publishers

Journal of Mechanics of Materials and Structures

Volume 14, No. 3

May 2019

-
- Experimental and numerical energy absorption study of aluminum honeycomb structure filled with graded and nongraded polyurethane foam under in-plane and out-of-plane loading**
ALIREZA MOLAIEE and SEYED ALI GALEHDARI 309
- Transient thermal stresses in a laminated spherical shell of thermoelectric materials**
YUE LIU, KAIFA WANG and BAOLIN WANG 323
- Tuning the propagation characteristics of the trapped and released strongly nonlinear solitary waves in 1-D composite granular chain of spheres**
BIN WU, HEYING WANG, XIUCHENG LIU, MINGZHI LI, ZONGFA LIU and CUNFU HE 343
- Accurate buckling analysis of piezoelectric functionally graded nanotube-reinforced cylindrical shells under combined electro-thermo-mechanical loads**
SHENGBO ZHU, YIWEN NI, JIABIN SUN, ZHENZHEN TONG, ZHENHUAN ZHOU and XINSHENG XU 361
- Thermoelastic fracture initiation: the role of relaxation and convection**
LOUIS M. BROCK 393
- Development of fracture mechanics model of beam retrofitted with CFRP plate subjected to cyclic loading**
SHAHRIAR SHAHBAZPANAH and HUNAR FARID HAMA ALI 413
- Assessment of degradation of railroad rails: finite element analysis of insulated joints and unsupported sleepers**
HOSSAM ELSAYED, MOHAMED LOTFY, HAYTHAM ZOHNAY and HANY SOBHY 429



1559-3959(2019)14:3;1-V